Hindawi
Advances in Polymer Technology
Volume 2023, Article ID 3114639, 8 pages
https://doi.org/10.1155/2023/3114639

Research Article

Preparation and Property Study of PA56/POE-g-MAH-GMA/PPO Ternary Alloy

Yunsheng Chong,[1,2] Liyan Wang,[1] Xiangming Xu,[2] Xiao Zhuang,[3] Rongrong Zheng,[1] Di Cao,[2] and Yanming Chen[1]

[1]*School of Petrochemical Engineering, Shenyang University of Technology, Liaoyang 111003, China*
[2]*Liaoyang Kangda Plastic Resin Co. Ltd., Liaoyang 111003, China*
[3]*Duke Kunshan University, Jiangsu 215316, China*

Correspondence should be addressed to Liyan Wang; wangliyan0122@163.com

Received 17 August 2023; Revised 9 October 2023; Accepted 17 November 2023; Published 5 December 2023

Academic Editor: Pierre Verge

Bio-based PA56 is as matrix resin, maleic anhydride (MAH), and glycidyl methacrylate (GMA) dual monomer grafted POE (POE-g-MAH/GMA) polyphenyl ether(PPO) are simultaneous as toughening agents. The PA56/POE-g-MAH-GMA/PPO ternary alloys containing 10 wt% POE-g-MAH-GMA with different PPO content prepared by the melt blending method through twin screw extruder. The structure and property of PA56/POE-g-MAH-GMA/PPO ternary alloys were studied. The results showed that the microscopic morphology of each alloy showed an obvious "sea-island" structure. PA56 is a continuous sea phase, and the island phase assumes the "core–shell structure," the etched POE-g-MAH-GMA particles are as the nucleus, and PPO are as the shell. When the PPO mass fraction is 30%, the relative crystallinity of the alloy is 11.56%, which is 1.68 times lower compared to the pure PA56, the alloy notch impact strength is 42.1 kJ/m^2, and reaches 11.7 times of pure PA56; the water absorption rate of 1.22%, which is 3.22 times lower than pure PA56.

1. Introduction

Polyamide is commonly known as nylon, a general term for polymers containing amide groups in the repeating units of the macromolecular backbone [1]. PA56 is a new bio-based polyamide synthesized from bio-based pentamethylene diamine and petroleum-based adipic acid [2, 3]. PA56 raw material bio-based pentamethylene diamine obtained by microbial fermentation of starch, which reduces the production costs of PA56, relieves the pressure of petroleum resource scarcity, and improves the product quality, making it a very competitive nylon material. The molecular structure of bio-based PA56 is similar to that of PA66, that is, there are some amide repeating units in the main chain of macromolecules, and the carboxyl and amino groups at the ends of the molecular chain [4–6]. Bio-based nylon PA56 has excellent mechanical properties, wear resistance, self-lubrication, and corrosion resistance, as well as good processability. However, PA56 has a obvious defects in engineering plastic applications. PA56 has higher water absorption rate and water absorption rate, lower impact strength, and poorer dimensional stability [7]. Thus, it is of great importance to improve the performance defects of PA56 (such as high-water absorption and low-impact strength), to partially or completely replace PA66 in automotive or electronic appliances, and to be widely used in the field of engineering plastics. In addition, with the increasing development of the market economy and the increasingly fierce competition of modern society, and higher requirements of the performance and the price of polymer materials, the alloy can more adapt to the requirements of the development of modern society compared with a single polymer [8, 9].

Nylon (PA) and polyphenylene ether (PPO) are two important of the five major engineering plastics [10]. PPO resin has excellent chemical stability, heat resistance, electrical properties, flame retardancy, and mechanical properties, etc. However, PPO has a fatal drawback of high-melt viscosity, which makes it difficult to process and mold, thus greatly limiting its application [11–15]. Nylon (PA) has many

advantages such as high strength, easy processing, and solvent resistance, etc. but its notched impact strength is low. To overcome the shortcomings of both PA and PPO, the alloy materials with the advantages of both were prepared and studied. Wu et al. [16, 17] prepared PA6/SEBS-g-MAH/poly-2,6-dimethyl phenyl ether (PPO) blends. While introducing the bulking agent styrene–maleic anhydride copolymer (SMA) and organically modified montmorillonite (OMMT) to obtain high strength, super tough, high strength, super tough, high-temperature resistant, and easy to process nanocomposite. Xu et al. [18] and Wang et al. [19] prepared a PPO/PA 6 alloy while introducing a bulking agent to chemically react the amino groups on nylon 6, which improved the interfacial bonding between POE particles and the matrix and significantly improved the dispersion of POE in the matrix. The diameter of the dispersed POE particles in the matrix was reduced substantially, leading to a significant toughening effect, and the above study better balanced the strength and toughness of PA6. Bio-based PA56/PPO as a new alloy maintains the advantages of good heat resistance, low hygroscopicity, and dimensional stability of PPO but also has the advantages of solvent resistance and good processing properties of PA, so that the properties of PA and PPO are complementary [20–22]. Blending and modifying these two engineering plastics can result in high-strength materials with balanced properties, where the advantages of one component can compensate for the disadvantages of other [23].

The high-water absorption of the new PA56 can negatively affect the toughness, strength, dimensional stability, and material processability, limiting the use of PA56 in practice to some extent. At present, there are few research reports on the modification of PA56 based on biological agents by scholars. POE-g-MAH-GMA toughened bio-based PA56 alloys were previously prepared by Chong et al. [24], and they have high toughness and low-water absorption properties. While the toughening effect is significant and outstanding, the rigidity of the alloy is not maintained. On this basis, a new method of toughening bio-based PA56 by design, utilizing a mixture of rubber particles and rigid particles instead of the traditional rubber particles for toughening, and bio-based PA56 was modified by melt blending to prepare PA56 alloys with excellent toughness and good rigidity. Thus, the PA56/POE-g-M A H-GMA/PPO ternary alloys containing 10 wt% POE-g-MAH-GMA with different PPO content were prepared by the melt blending method through twin screw extruder in this paper. This article investigates the effects of PPO content on the microstructure, mechanical properties, water absorption, rheological properties, and thermal properties of the ternary alloys. At the same time, explore the relationship between their structure and properties. This study provides a reference for the modification and practical application of the bio-based PA56 alloy.

2. Experiment

2.1. Main Raw Materials

Bio-based nylon 56 (PA56, model E-2260): 45% of carbon is from biological sources, with a viscosity of 2.7–2.8, intrinsic flame retardant properties, produced by Kaisai (Wusu) Biomaterials Co., Ltd.;

Polyphenylene oxide (PPO, model NF5300): Guangzhou Jusailong Co., Ltd.;

Compatibilizer POE-g-MAH-GMA: self-made (melt blending grafting method);

Compatibilizer PPO-g-MAH: Shenyang Ketong Plastic Co., Ltd.;

other additives: commercially available.

2.2. Main Instruments and Equipment

Electric blast drying oven: GT-SN-7005, Taiwan High Speed Rail Testing Instrument Co., Ltd.;

Twin screw extruder: SHJ-42, diameter 40 mm, aspect ratio 40 : 1, Nanjing Jieya Extrusion Equipment Co., Ltd.;

Injection molding machine: HST-1300, Ningbo Haitian Plastic Machinery Manufacturing Co., Ltd.;

Ultralow temperature scanning electron microscope, SEM, Sigma 300, Carl Zeiss.;

Impact specimen chamfering machine: GT-7016-A3, Taiwan High Speed Rail Testing Instrument Co., Ltd.;

Digital impact testing machine: GT-7045-MDL, Taiwan High Speed Rail Testing Instrument Co., Ltd.;

Servo controlled tensile testing machine: AI-7000MI, Taiwan High Speed Rail Testing Instrument Co., Ltd.;

Analytical balance: JA1003N-5003N, Qingdao Juchuang Environmental Protection Co., Ltd.;

Thermal analyzer (DSC): DSC-822e, Mettler Toledo, Switzerland.

2.3. Preparation of PA56/POE-g-MAH-GMA/PPO Alloy Samples. The PA56 slices and PPO were dried enough, mixed with POE-g-MAH/GMA and other additives in a high-speed mixer, and then the PA56/POE-g-MAH-GMA/PPO series alloy was prepared by the melt blending process route of twin-screw extruder. The temperatures of Zone 1–Zone 12 of the twin screw extruder were set at 230, 240, 250, 265, 275, 275, 265, 260, 255, 250, 245, and 250°C, respectively, with a screw speed of 400 rpm. Then, the sample slices are prepared by cutting the particles. The mass fractions of PPO in the alloy samples are 0%, 10%, 20%, and 30%, respectively. Correspondingly, the samples are recorded as PA56, PA56/POE-g-MAH-GMA/PPO-1#, PA56/POE-g-MAH-GMA/PPO-2#, and PA56/POE-g-MAH -GMA/PPO-3#.

2.4. Preparation of PA56/POE-g-MAH-GMA/PPO Alloy Test Strips. The PA56/POE-g-MAH-GMA/PPO alloy slices were dried in a dry oven at 105°C for 6 hr. The sample strips required for the mechanical property testing were then prepared by an injection molding machine. This injection molding process parameters include injection temperatures of 245, 260, and 255°C in the first to third zones, cooling time of 16 s, injection pressure of 45 MPa, and back pressure of 10 MPa, followed by performance testing. The sample

strips were placed at a temperature of 23 ± 2°C and humidity of 50% ± 5% for 24 hr before the performance tests.

2.5. Structural Characterization and Performance Testing

2.5.1. Cross-Section Morphology. The microstructure of the cross-section of the alloy spline observed by an ultralow temperature scanning electron microscope. In order to maintain the original phase morphology of the alloy, the spline is immersed in liquid nitrogen, and the low-temperature brittle fracture is carried out after the spline reaches Thermal equilibrium (about 30 min). In order to clearly observe the structure of the dispersed phase, the cross-section was etched with *n*-heptane at 60°C for 12 hr to remove POE. Finally, before SEM testing, spray gold treatment is performed on the cross-section. SEM testing was conducted at a working voltage of 3.0 kV and an accelerating voltage of 10.0 kV.

2.5.2. DSC Test. N2 atmosphere, heating from 25 to 290°C at a rate of 10°C/min, holding constant temperature for 5 min to eliminate historical heat, and then cooling to 25°C at a rate of 10°C/min to obtain the sample heating and cooling curves. The crystallinity of the alloy is expressed by the ratio of the melting heat of the material to the theoretical melting heat of complete crystallization, and the calculation formula is as follows:

$$X_C = \frac{\Delta H_m}{\Delta H_m{}^0} \times 100\%, \quad (1)$$

where X_C—crystallinity, %; ΔH_m—Heat of melting of the substance, J/g; ΔH_m^0—Theoretical heat of melting for complete crystallization, taken as 188.7 J/g [25–26].

2.5.3. Impact Strength. The simple beam impact performance of PA56/PPO alloy samples was tested using a dynamic impact analyzer, in accordance with the GB/T 1043.1-2008 standard.

2.5.4. Tensile and Bending Performance. The tensile and bending performance of the sample is tested using a servo controlled tensile testing machine. The tensile performance test follows the GB/T 1040-2018 standard, and the bending performance test follows the GB/T 9341-2008 standard.

2.5.5. Water Absorption Test. The international standard test tensile samples were weighed using analytical balance to obtain the mass m_1, and then immersed in water at 23 ± 2°C and 50% ± 5% humidity conditions for 72 hr, then taken out and wiped dry, then weighed to obtain the mass m_2. The water absorption of test alloy strips was calculated by the formula:

$$C = (m_2 - m_1)/m_1 \times 100\%. \quad (2)$$

2.5.6. Melt Mass FLow Rate (MFR). The plastic Melt Flow Index Tester (GT-7100-MI, Taiwan High Speed Rail) is tested according to GB/T 3682-2000, with a temperature of 285°C and load of 2.16 kg. The average value of each group of samples is taken after five tests.

3. Results and Discussion

3.1. SEM Microscopic Morphology of PA56/POE-g-MAH-GMA/PPO Alloy Cross-Section. Figure 1 shows the SEM pictures of PA56 and PA56/POE-g-MAH-GMA/PPO alloys cross-sections with different contents of PPO.

As can be seen from Figure 1, the microscopic morphology of the PA56/POE-g-MAH-GMA/PPO alloy shows an obvious "sea-island" structure, PA56 is a continuous sea phase, and the island phase shows a "core–shell structure" with the etched POE-g-MAH-GMA particles as the core and PPO as the shell. The nuclei in the island phase appear in the form of small circular voids, which are distributed in a uniform and regular spherical particle shape in the island phase, and the core domain is about 100–150 nm. Its analyzed that the tested PA56/POE-g-MAH-GMA /PPO alloys cross sections were all etched with *n*-heptane at 60°C for 12 hr, and POE-g-MAH/GMA was removed because it is soluble in *n*-heptane. Thus, the small hollow hole was caused by removed POE-g-MAH-GMA in the SEM microscopic morphology of the alloys. This analysis is in agreement with that in the fomer paper published by our team [24]. In addition, it is easy to see that the core–shell island phase uniformly disperses in the PA56 marine phase. This structure endows the alloy with good toughness and maintains the rigidity, the type of alloy to achieve the effect of rigidity and toughness balances with the increase of PPO dosage, the core–shell island size gradually increases, but the size of POE-g-MAH-GMA as the core of the island phase remains unchanged.

3.2. Effect of PPO Content on the Melt Crystallization of PA56/POE-g-MAH-GMA/PPO Alloys. Figure 2 is irrespectively DSC nonisothermal crystallization cooling curves and secondary heating melting curves of PA56/POE-g-MAH-GMA/PPO alloys. The thermal performance parameters of PA56/POE-g-MAH-GMA/PPO alloys are listed in Table 1.

It can be seen from Figure 2 and Table 1 that the crystallization temperature T_c of PA56/POE-g-MAH-GMA/PPO alloys decreases from 233.06 to 231.61°C, and the relative crystallinity X_c decreases from 19.46% to 11.56% when the addition amount of PPO increases from 10% to 30%. This is because PPO is a noncrystalline resin, and the molecular chain contains a large number of rigid aromatic ring structures, which destroys the overall order structure degree of the alloy and reduces the crystallization ability of the alloy macromolecule. At the same time, the addition of PPO hinders the mobility of the alloy, the alloy macromolecule needs a longer time to arrange into the lattice, which leads to the decrease of T_c of the alloy as the increase of content of PPO. However, the melting temperature T_m of the PA56/POE-g-MAH-GMA/PPO alloys changes a little. This is because T_m is the characteristic temperature of PA56 crystal, only relative to PA56 crystal structure.

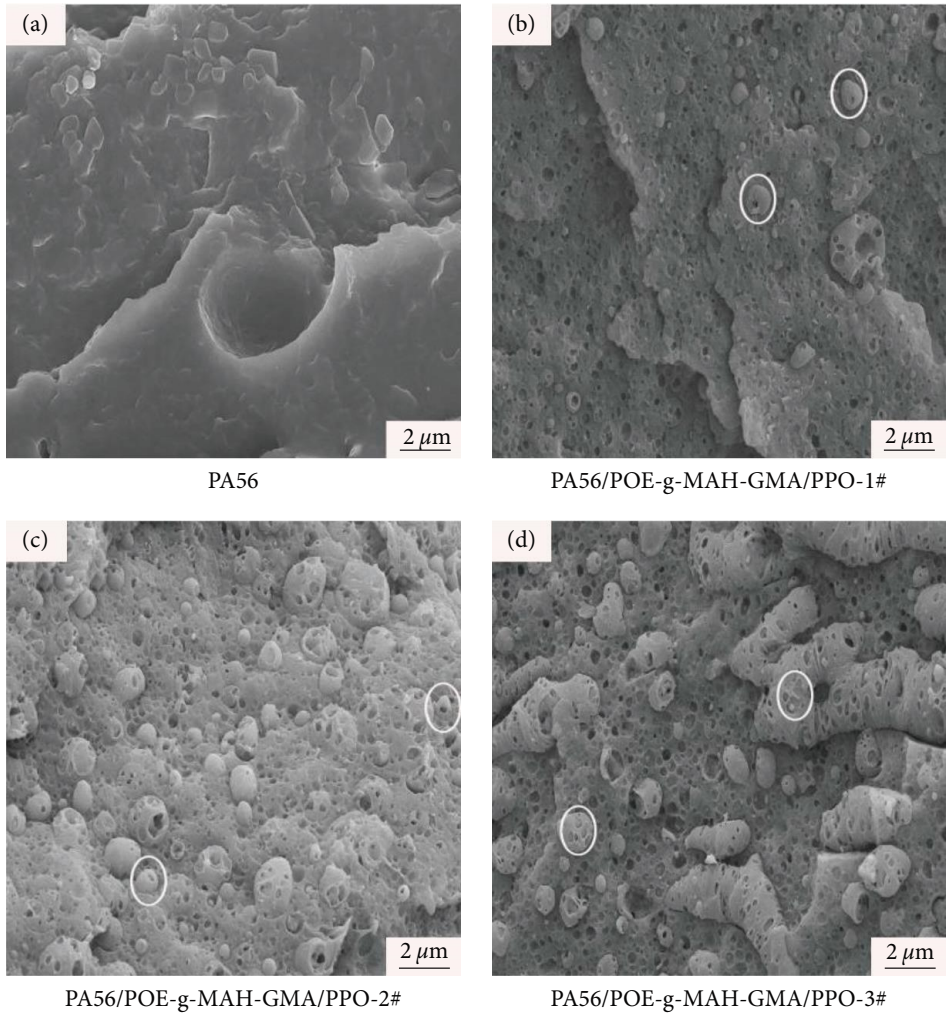

Figure 1: SEM micromorphology of PA56 and PA56/POE-g-MAH-GMA/PPO alloys (a–d).

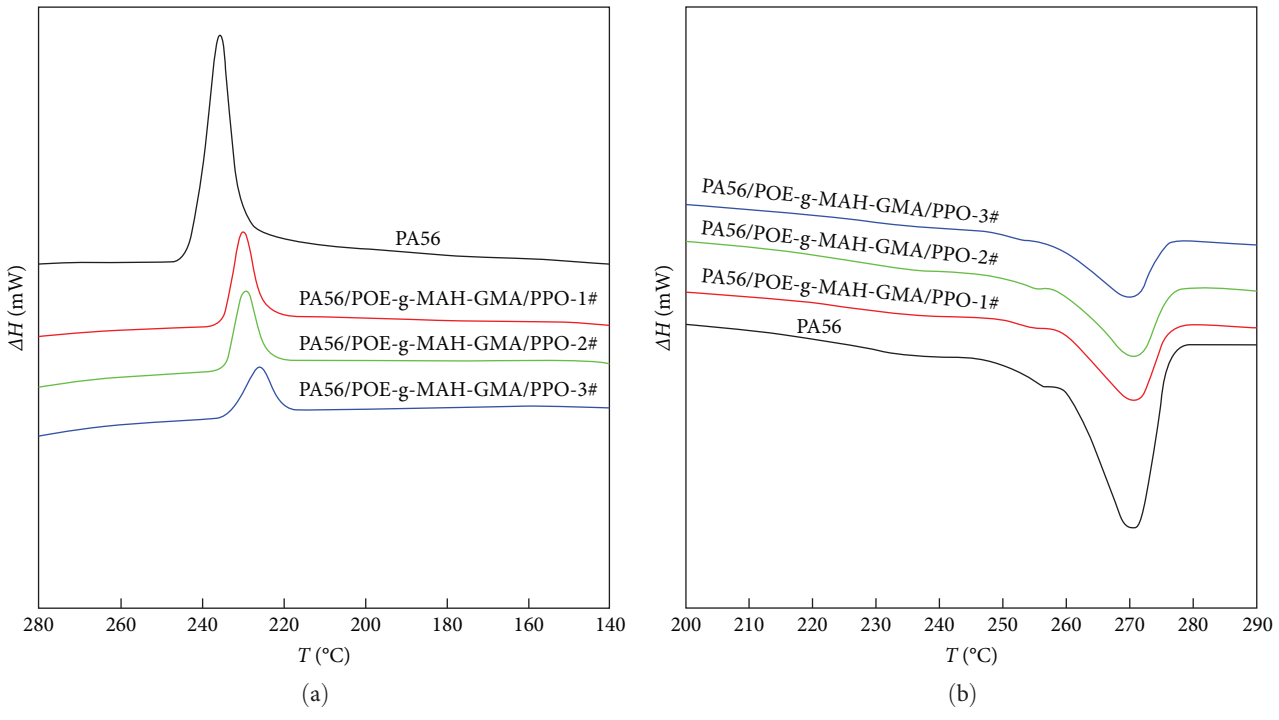

Figure 2: DSC nonisothermal crystallization cooling curves (a) and secondary heating curve (b) of PA56/POE-g-MAH-GMA/PPO alloys.

Table 1: Thermal property parameters of PA56/POE-g-MAH-GMA/PPO alloys.

Sample	T_c (°C)	ΔH_c (J·g^{-1})	T_m (°C)	ΔH_m (J·g^{-1})	X_c (%)
PA56	235.83	30.81	270.45	36.58	19.46
PA56/POE-g-MAH-GMA/PPO-1#	233.06	23.94	271.05	31.54	16.78
PA56/POE-g-MAH-GMA/PPO-2#	233.01	22.03	270.24	28.77	15.30
PA56/POE-g-MAH-GMA/PPO-3#	231.61	17.37	270.20	21.74	11.56

Note. T_m is the melting temperature; T_c is the cooling crystallization temperature; ΔH_c is the enthalpy of melting; and X_c is the relative crystallinity.

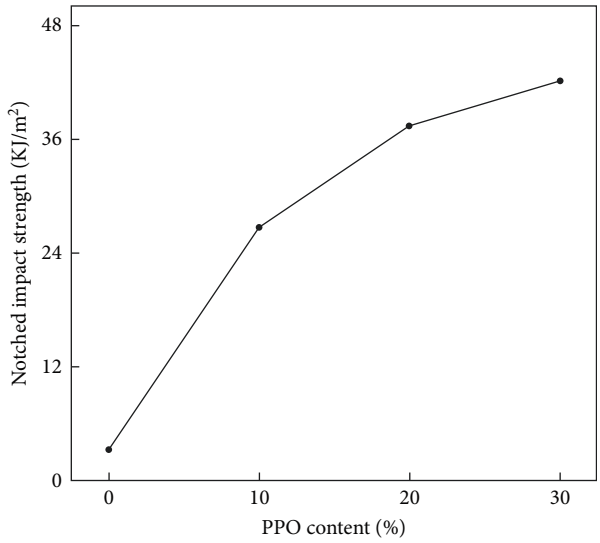

Figure 3: Effect of PPO content the notch impact strength on PA56/POE-g-MAH-GMA/PPO alloys.

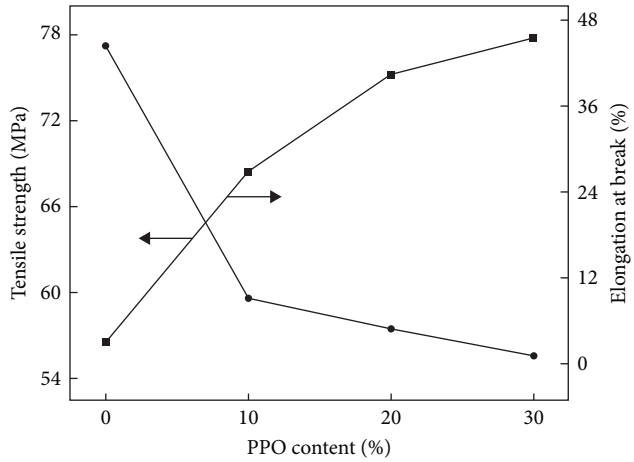

Figure 4: Effect of PPO content on tensile properties of PA56/POE-g-MAH-GMA/PPO alloy.

3.3. Effect of PPO Content on the Mechanical Properties of PA56/POE-g-MAH-GMA/PPO Alloys

3.3.1. Impact Performance. The relation curves of the simple support beam notch impact strength of PA56/POE-g-MAH-GMA/PPO alloy samples with PPO content are shown in Figure 3.

As can be seen from Figure 3, the PA56/POE-g-MAH-GMA/PPO alloy prepared by the team in this paper contains 10% POE-g-MAH-GMA and different mass fractions of PPO. The notched impact strength of PA56/POE-g-MAH-GMA/PPO alloy is 26.7 kJ/m^2 when the PPO content is 10%, and the impact strength of the alloy is 42.1 kJ/m^2 when the PPO content is 30%, which is 11.7 times higher than that of pure PA56. According to our previously written paper [24], the notched impact strength of PA56/POE-g-MAH-GMA alloy containing 10% POE-g-MAH-GMA is 16.7 kJ/m^2.

In comparison with these data, it is proved that the two toughen agents work synergisticly. This is, on the one hand, because the side group MAH and epoxy group in the POE-g-MAH/GMA, and PPO-g-MAH molecular chain react, respectively, with the amino group and carboxyl group in the PA 56 macromolecular chain, which makes a strong interaction between the elastomeric POE, PPO, and PA56, and this increases the interfacial bond between the polymers in the alloy. On the other hand, when the PA56/POE-g-MAH-GMA/PPO alloy is impacted, the elastomer POE as a stress concentrator can induce a large number of crazings in the PA56 matrix, and the stress field of the crazings' tip can induce the generation of shear bands, and the shear bands can prevent the further development of crazings, and the generation and development of crazings and shear bands consume a lot of energy, so impact strength of the alloy increases. At the same time, rigid PPO particles toughen PA56 in the mechanism of cold drawing. That is, when the PA56/POE-g-MAH-GMA/PPO alloy is impacted, static pressure is generates on the equatorial plane of the dispersed phase PPO, A large static pressure generated on the equatorial surface of the PPO dispersed phase, which makes the PPO particles easy to yield and produce plastic deformation, absorbing a large amount of impact energy, so that the impact strength of the alloy gap gradually increases gradually with the increase of PPO content. In general, both the crazing-shear band mechanism of elastomer and rigid particle cold drawing mechanism interprets synergistic toghening appearance of POE-g-MAH/GMA and PPO.

3.3.2. Tensile and Flexural Properties. The relationship curves of PA56/POE-g-MAH-GMA/PPO alloy samples' tensile strength and elongation at break with PPO content are shown in Figure 4, and the relationship curves of their bending strength and bending modulus with POE-g-MAH/GMA content are shown in Figure 5.

As can be seen from Figures 4 and 5, the tensile strength, flexural strength, and flexural modulus of the alloys decreased with the increase of PPO addition, while the elongation at break showed an increasing trend. This may be due to the

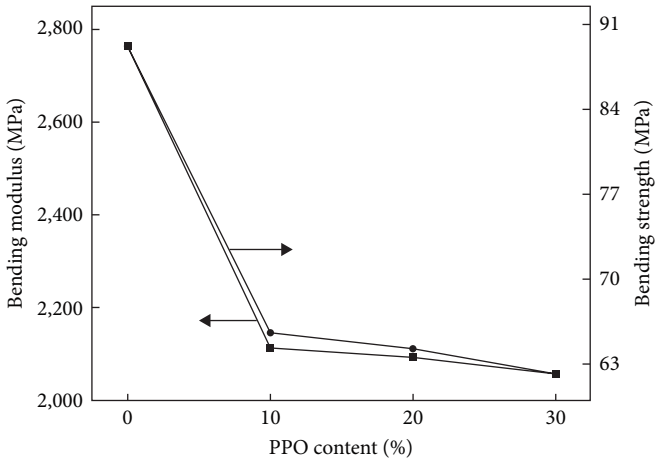

Figure 5: Effect of PPO content on flexural properties of PA56/POE-g-MAH-GMA/PPO alloy.

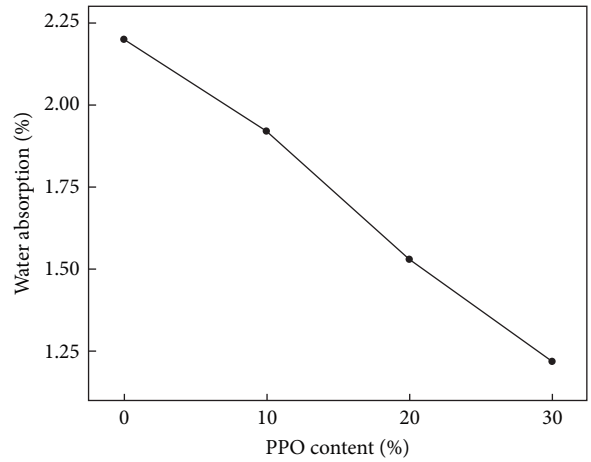

Figure 6: Effect of PPO content on water absorption of PA56/POE-g-MAH-GMA/PPO alloy.

incompatibility of the two, there is a certain interfacial tension, resulting in weak interfacial bonding between the two. Thus, with the content of PPO increase, the interface force affects the ternary alloy rigidity more obviously.

Compared the data of the tensile strength and flexural properties of PA56/POE-g-MAH-GMA/PPO ternary alloys and that of PA56/POE-g-MAH-GMA binary alloys [24], the tensile strength of ternary alloys changes slightly, however, flexural strength and flexural modulus of the ternary alloys all changes better. This is due to the presence of a rigid benzene ring structure in the PPO molecular chain, compared with other engineering materials, PPO's rigidity, modulus, and tensile strength are better. Thus, it can be concluded that the addition of PPO make ternary alloy have good rigidity which affords to our design idea.

3.4. Water Absorption. The change curves of the water absorption of PA56/POE-g-MAH-GMA/PPO alloy samples with the different PPO content are shown in Figure 3.

As can be seen from Figure 6, the water absorption of the PA56/POE-g-MAH-GMA/PPO alloy material decreases gradually with the increase of PPO content. The water absorption rate of the pure PA56 sample is as high as 3.94% after immersing in water for 72 hr. When the PPO addition is 10%, the water absorption rate of the alloy material is 1.92%, which is 2.05 times lower than that of the pure PA56 sample; when the PPO addition is 20%, the water absorption rate of the alloy material is 1.53%, which is 2.57 times lower than that of the pure PA56 sample; when the PPO addition is 30%, the water absorption rate of the alloy material is 1.22%, which is 3.22 times lower than that of the pure PA56 sample. The study shows that the addition of PPO can better improve the water absorption of PA56 and reduce the negative effects of high-water absorption. The water absorption of PA56/POE-g-MAH-GMA/PPO alloy decreases with the increase of PPO content. This is due to the fact that there is no water-absorbing group in the molecular structure of polyphenylene ether, so the alloy has lower water absorption.

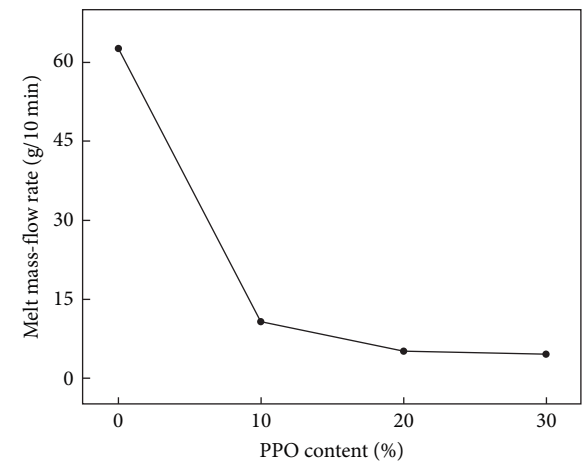

Figure 7: Effect of PPO content on mass-flow rate of PA56/POE-g-MAH-GMA/PPO alloy melt.

3.5. Melt Mass FLow Rate (MFR). The change curves of the melt MFR of PA56/POE-g-MAH-GMA/PPO alloy samples with the different PPO content are shown in Figure 7.

From Figure 7, it can be seen that with the increase of PPO content, the melt flow rate of PA56/PPO alloy material gradually decreases, resulting in a decrease in the forming and processing performance of the alloy. This is due to the high viscosity of PPO melt and the existence of aromatic ring in the molecular structure, which makes it difficult to move in the molecular chain, resulting in the poor fluidity.

4. Conclusion

(1) PA56/POE-g-MAH-GMA /PPO alloy shows an obvious "sea-island" structure, PA56 is a continuous sea phase, and the island phase shows a "core-shell structure" with the etched POE-g-MAH-GMA particles as the core and PPO as the shell. The nuclei in the island phase appear in the form of small circular voids, which are distributed in a uniform and regular

spherical particle shape in the island phase, and the core domain is about 100–150 nm. This structure endows the alloy with good toughness and maintains the rigidity, the type of alloy to achieve the effect of rigidity and toughness balances.

(2) When the mass fraction of PPO is 30%, the notched impact strength is 42.1 kJ/m^2 at room temperature, which is 11.7 times that of pure PA56. It shows that the toughness of the alloy is significantly improved; when the mass fraction of PPO is 30%,the water absorption rate of 1.22%, which is 3.22 times lower than the pure PA56. With the increase of PPO, the water absorption rate of PA56 gradually decreases, and the addition of PPO reduces the negative impact of PA56's high water absorption rate. At the same time, the tensile strength, bending strength, and melt flow rate showed a small decreasing trend.

(3) The crystallization temperature T_c of PA56/POE-g-MAH-GMA/PPO alloys decreased from 233.06 to 231.61°C. And the relative crystallinity X_c decreased from 19.46% to 11.56% when the addition amount of PPO increased from 10% to 30%.

Data Availability

The authors declare that the data supporting the findings of this study are available within the article.

Conflicts of Interest

The authors declare that they have no conflicts of interest.

References

[1] Y. Zhao, L. Wang, Y. Chong, Y. Chen, R. Zheng, and L. Zhang, "Preparation and properties of glass fiber reinforced nylon56 composites," *Polymer Composites*, vol. 43, no. 9, pp. 6660–6666, 2022.

[2] Y. L. Li, X. M. Hao, Y. F. Guo, X. Chen, Y. Yang, and J. M. Wang, "Study on the acid resistant properties of bio-based nylon 56 fiber compared with the fiber of nylon 6 and nylon 66," *Advanced Materials Research*, vol. 1048, pp. 57–61, 2014.

[3] A. Gao, H. Zhang, G. Sun, K. Xie, and A. Hou, "Light-induced antibacterial and UV-protective properties of polyamide 56 biomaterial modified with anthraquinone and benzophenone derivatives," *Materials & Design*, vol. 130, pp. 215–222, 2017.

[4] Y. Wang, Y. Zhang, Y. Xu, X. Liu, and W. Guo, "Research on compatibility and surface of high impact bio-based polyamide," *High Performance Polymers*, vol. 33, no. 8, pp. 960–968, 2021.

[5] Y. A. Eltahir, H. A. M. Saeed, Y. Xia, H. Yong, and W. Yimin, "Mechanical properties, moisture absorption, and dyeability of polyamide 5,6 fibers," *The Journal of The Textile Institute*, vol. 107, no. 2, pp. 208–214, 2016.

[6] Y. Zhang, Y. Wang, Y. Xu, X. Liu, and W. Guo, "Modification of biobased polyamide 56 to achieve ultra-toughening," *Polymer-Plastics Technology and Materials*, vol. 60, no. 14, pp. 1–20, 2021.

[7] C. Xue, K.-M. Hsu, C.-Y. Chiu, Y.-K. Chang, and I.-S. Ng, "Fabrication of bio-based polyamide 56 and antibacterial nanofiber membrane from cadaverine," *Chemosphere*, vol. 266, Article ID 128967, 2021.

[8] M. Shen and H. Kawai, "Properties and structure of polymeric alloys," *AIChE Journal*, vol. 24, no. 1, pp. 1–20, 1978.

[9] A. Kato, M. Nishioka, Y. Takahashi et al., "Phase separation and mechanical properties of polyketone/polyamide polymer alloys," *Journal of Applied Polymer Science*, vol. 116, no. 5, pp. 3056–3069, 2010.

[10] Y. T. Zhang, Y. Li, L. Li, and X. W. Qu, "The study on the preparation and properties of PPO/PA66 alloy with a new type of compatibtlizer B," *Key Engineering Materials*, vol. 501, pp. 99–103, 2012.

[11] S. A. Tagliavini, A. Y. Mikawa, H. Yamanaka, F. Henrique-Silva, and P. I. Costa, "Polysiloxane-poly (propylene oxide) hybrid discs as solid phase in anti-HCV detection using a recombinant core protein," *Talanta*, vol. 75, no. 2, pp. 461–465, 2008.

[12] P. P. Chu, J.-M. Huang, H.-D. Wu, C.-R. Chiang, and F.-C. Chang, "Molecular dynamics and mechanical properties correlations of PA6/PPO blends compatibilized with SMA," *Journal of Polymer Science Part B*, vol. 37, no. 11, pp. 1155–1163, 1999.

[13] H. Yu, Y. Zhang, and W. Ren, "Effect of EVM/EVA-g-MAH ratio on the structure and properties of nylon 1010 blends," *Journal of Polymer Science, Part B. Polymer Physics*, vol. 47, no. 9, pp. 877–887, 2009.

[14] S. J. Wu, T. K. Lin, and T. K. Shyu, "Cure behavior, morphology, and mechanical properties of the melt blends of epoxy with polyphenylene oxide," *Journal of Applied Polymer Science*, vol. 75, no. 1, pp. 26–34.

[15] L. Weng, Y. Zhang, X. Zhang, L. Liu, and H. Zhang, "Synthesis and properties of cyanate mixed resin systems modified by polyphenylene oxide for production of high-frequency copper clad laminates," *Journal of Materials Science: Materials in Electronics*, vol. 29, pp. 2831–2840, 2018.

[16] Y. Wu, H. Zhang, B. Shentu, and Z. Weng, "Preparation of poly (phenylene oxide)/polyamide-6 nanocomposites with high tensile strength and excellent impact performance," *Industrial & Engineering Chemistry Research*, vol. 54, no. 22, pp. 5870–5875, 2015.

[17] Y. J. Wu, L. Q. Dal, and B. Q. Shentu, "Toughening effects of "core-shell" particles in PA6/SEBS-g-MA/PPO blends," *Journal of Chemical Engineering of Chinese Universities*, vol. 31, no. 6, pp. 1327–1332, 2017.

[18] X. L. Xu, X. Y. Cheng, X. N. Sun, S. E. Y. ang, and Tianjin Changlu Haijing Group Co., Ltd., "Development of PA6/PPO nylon alloy," *Journal of Salt and Chemical Industry*, vol. 45, no. 5, pp. 17–20, 2016.

[19] X. D. Wang, Q. Zhang, and R. G. Jin, "Performance of PPO/nylon 6 alloy toughened with maleic anhydride functionalized POE," *Chinese Journal of Materials Research*, vol. 2, pp. 193–199, 2002.

[20] Z. H. Guo, Y. Shen, Y. Wu, and Z. P. Fang, "Reactive compatibilization of poly(phenylene oxide)/polyamide 6 blended with poly (phenylene oxide) grafted glycidyl methacrylate copolymer," *Polymer Materials Science & Engineering*, vol. 28, no. 11, pp. 84–88, 2012.

[21] Z. Zhang, K. Cai, S. Liu et al., "The effect of HIPS-g-MAH on the mechanical properties of PA66/PPO alloy," *Polymer Bulletin*, pp. 1–13, 2021.

[22] J.-S. Lin, M.-H. Chung, C.-M. Chen, and M. O. Liu, "Thermal characterization, melting behaviors, dynamic mechanical properties, and morphology in the polymorphism of syndiotactic

polystyrene and poly (2, 6-dimethyl-1, 4-phenylene oxide)," *Journal of Non-Crystalline Solids*, vol. 355, no. 34-36, pp. 1698–1702, 2009.

[23] X. Wang, W. Feng, H. Li, and R. Jin, "Compatibilization and toughening of poly (2, 6-dimethyl-1, 4-phenylene oxide)/ polyamide 6 alloy with poly (ethylene 1-octene): mechanical properties, morphology, and rheology," *Journal of Applied Polymer Science*, vol. 88, no. 14, pp. 3110–3116, 2003.

[24] Y. Chong, X. Zhuang, C. Guan, L. Wang, R. Zheng, and Z. Bie, "Preparation and performance study of POE-g-MAH/GMA toughened bio-based PA56 alloys," *Journal of Alloys and Compounds*, vol. 960, Article ID 170813, 2023.

[25] J. Puiggalí, L. Franco, C. Alemán, and J. A. Subirana, "Crystal structures of nylon 5, 6. A model with two hydrogen bond directions for nylons derived from odd diamines," *Macromolecules*, vol. 31, no. 24, pp. 8540–8548, 1998.

[26] K. R. I. J. S. W. I. J. K. van, H. E. N. Bersee, W. F. Jager, and S. J. Picken, "Optimisation of anionic polyamide-6 for vacuum infusion of thermoplastic composites: choice of activator and initiator," *Composites Part A: Applied Science and Manufacturing*, vol. 37, no. 6, pp. 949–956.